

Electric Propulsion Vacuum Chamber Design Approaches for Reducing Sputtering Effects

IEPC-2024-187

*Presented at the 38th International Electric Propulsion Conference, Toulouse, France
June 23-28, 2024*

Graeme Sabiston*

University of California, Los Angeles, Los Angeles, CA, 90095, USA

Richard E. Wirz^{†‡}

*University of California, Los Angeles, Los Angeles, CA, 90095, USA
Oregon State University, Corvallis, OR, 97331, USA*

A novel particle tracking simulation framework provides insight into the mitigation and control of sputtering effects in electric propulsion (EP) vacuum chambers. Monte-Carlo simulations of ions and sputtered atoms are physically informed by binary-collision approximation data, and are utilized to model the behavior of sputterants within EP test facilities. The impact of volumetrically complex materials (VCMs) on reducing unwanted sputterant deposition on critical surfaces is then explored, as VCMs demonstrate significantly decreased sputter yields compared to traditional materials. The selection of the type of VCM, and their placement locations throughout the chamber were found to be critical, as certain VCM implementations can increase sputterants to critical surfaces. Actionable insights for optimizing EP test chambers are provided, contributing to the development of more reliable in-space propulsion systems.

I. Motivation and Background

Electric propulsion (EP) test facilities are an integral part of the testing and development campaigns of in-space propulsion devices and admit the opportunity to accurately predict thruster performance and lifetime prior to deployment. While there are several limitations that arise when attempting to adequately mimic a space environment, one of the largest contributors is the contamination of the plasma, test chamber, and thruster with sputterants produced by plasma-material interactions (PMI). Test facility walls and beam targets are commonly lined with low-sputter yield carbon compounds to reduce the severity of PMI facility effects, however, experiments still show deposition, layering, and flaking of films that have been deposited onto thruster and facility surfaces.¹ Additionally, these sputterants can cause underestimation in grid erosion for gridded-ion thrusters,² and interfere with plasma diagnostics by coating insulating surfaces and increasing probe collection area.³ With the advent of higher thrust propulsion EP devices, the efficacy of current mitigation techniques may be insufficient, thereby hampering the development of the next generation of in-space propulsion. The choice of a suitable beam target, and the overall chamber design, is therefore imperative to minimize the sputtering of unwanted atomic species in test chambers that would otherwise pollute the test environment. Indeed, multi-institutional efforts sponsored by NASA are currently underway (e.g., Joint Advanced Propulsion Institute, JANUS⁴) to explore advanced mitigation strategies for high-power EP devices, with one of the main focuses being minimizing sputtering.

Some of the most comprehensive modeling efforts devoted to simulating sputtering in vacuum systems have used hybrid PIC-Direct Simulation Monte Carlo (DSMC) methods to simulate the plasma conditions

*PhD Candidate, Mechanical and Aerospace Engineering, graemes1@ucla.edu

†Adjunct Professor, Mechanical and Aerospace Engineering, wirz@ucla.edu

‡Boeing Professor, Executive Director of Aerospace Research Programs, College of Engineering, richard.wirz@oregonstate.edu

and sputterants,⁵⁻⁹ with some additional efforts focused on radiosity view-factor modeling approaches.¹⁰ We seek to develop a computationally efficient particle tracking simulation environment that supplements these existing efforts in a number of ways: Firstly, data from binary collision approximation (BCA) simulations are used in order to capture the complexities of the sputterant probability density functions (PDFs) and sputter yield distributions, compared to analytical formulations such as Yamamura.¹¹ Next, we explore the effect of sputtering interactions with non-beam target chamber surfaces, which will be shown to have a large impact on the total sputtered material in the vacuum facility. Finally, we investigate how beam targets composed of volumetrically complex materials (VCMs), which suggest favourable plasma-facing performance, can reduce facility effects.^{12,13}

Rather than developing a PIC-DSMC framework that solves for the plasma physics and plume characteristics in the test facility, the scope of this effort is to use a reduced-order model to simulate the ballistic sputtering physics as a method to accurately track the creation and transport of sputterants. This particle tracking approach does not rely on the solutions of coupled field equations throughout a discretized computational domain, instead simply computing the ballistic motion of ions and sputtered particles; these simplifications, such as assuming a non-collisional plume, dramatically reduces the computational workload. We therefore aim to use this framework as a robust tool to determine strategies from the perspective of beam target and chamber design to aid in minimizing the effects of sputtering on EP thruster testing campaigns.

II. Sputtering Theory

Utilizing the widely used, experimentally verified Monte-Carlo BCA code, TRI3DYN,¹⁴ ion-solid interaction data is generated for multiple projectile-target material combinations, and varying ion energies and incidence angles. The raw data is then processed to produce statistical distributions of sputter yield and sputterant trajectory PDFs. This data informs the sputtering physics and equations of motion for a particle tracking simulation code; for each interaction between an ion and a solid surface, two distinct weighted probability calculations are completed to determine the integer quantity of sputterants produced, and the unit vector(s) of sputterant direction from the target surface (see Fig. 1). By utilizing TRI3DYN, we aim to increase the accuracy of the PDFs and sputter yield distributions compared to generalized analytical functions, including effects such as single-knock-on peaks and specific material dependent effects.

A. Volumetrically Complex Materials

VCMs are innovative open-cell structures that have demonstrated to be up to ten times more resistant to sputtering in extreme plasma conditions.¹⁵ This advancement could significantly extend the lifespan of essential components in fusion and space propulsion systems. VCMs benefit from a “bend-but-don’t-break” property, which allows them to absorb the energetic plasma species without experiencing catastrophic micro-scale cracking and sputtering or large-scale failures that affect conventional materials. The key to the sputter-resistance of VCMs in plasma-facing environments lies in a process known as geometric trapping. When the ligaments of a VCM are sputtered, many of the dislodged atoms reattach to nearby ligaments before they are allowed to escape the structure. This re-adhesion prevents the atoms from escaping, thereby enhancing the material’s resistance to sputtering over the lifetime of the VCM. The geometric trapping ability of stochastic foam VCMs with relative densities between 8% and 30% has been found to reduce the sputter yield by 40% to 60%.^{13,15} Additionally, stochastic carbon foam VCMs have been shown to reduce secondary electron emission (SEE), which is responsible for degradation of plasma-facing surfaces and plasma instabilities, by up to 35%.¹⁶ While research is limited on the topic, reductions in ion-induced electron emission can be expected by similar mechanisms to SEE.^{17,18}

Two types of carbon VCMs, with different PDFs, are considered in this study. Stochastic carbon foam VCMs, as described in Li and Wirz (2021),¹⁵ have PDFs of sputterant trajectory that resemble that of flat materials at normal incidence, of the same elemental composition. This result is displayed in Fig. 2, where PDF data from a sputtering experiment wherein a tungsten VCM of 65% relative density (RD), with 65 pores-per-inch (PPI) was bombarded with 150eV xenon ions shows to align well with TRI3DYN results of flat tungsten. Additional VCM sputtering experiments have demonstrated similar findings for micro-architected molybdenum structures.¹⁹ This effect is analogous to the concept of accommodation coefficient in surface science, wherein gas molecules scatter in random directions after colliding with the

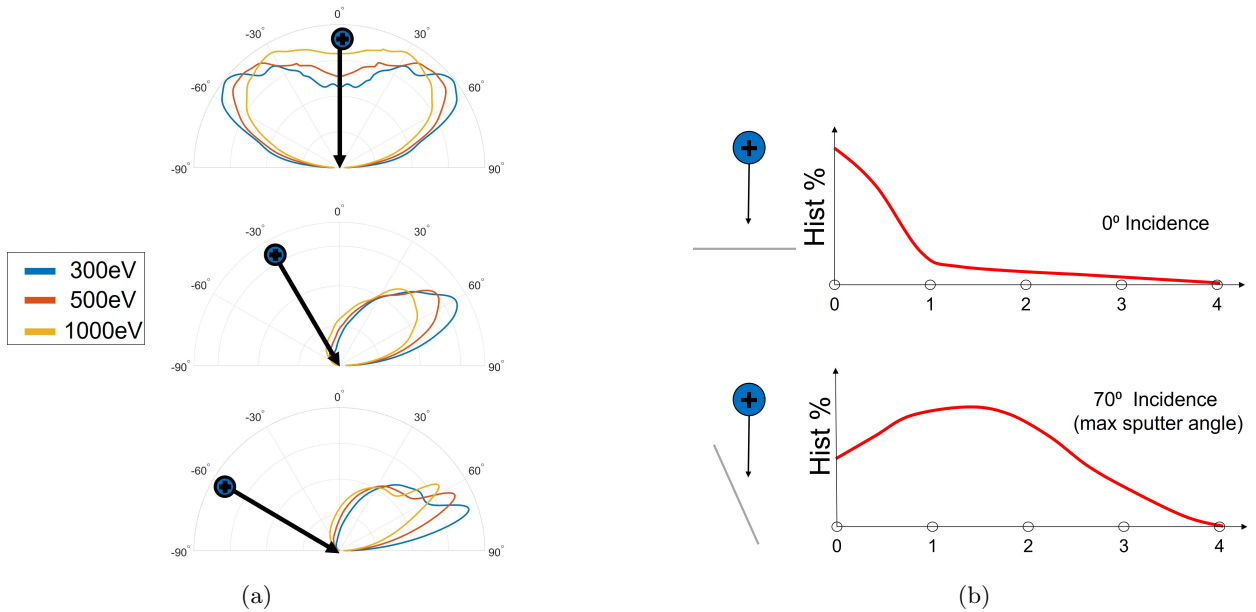


Figure 1: a) PDFs for carbon sputterant trajectories at varying xenon ion incidence angles and energies, generated by TRI3DYN. b) Weighted probability function of angle-dependent sputter yield is necessary to determine appropriate sputter yield for a given ion-solid interaction. Figures adapted from Sabiston and Wirz (2024).¹³

surface, regardless of the angle of incidence.²⁰ Due to their isotropic nature, stochastic VCMs produce a high accommodation coefficient, serving to eliminate the directionality information of the incident ions when interacting with the VCM, leading to a symmetric, under-cosine PDF normal to the VCM surface. As an alternative to stochastic carbon foam VCMs, regularized, uniform geometries created via metal additive manufacturing have shown promise as robust plasma-facing materials.²¹ Sabiston and Wirz developed 316L stainless steel cage-like VCMs, composed of ligaments with triangular cross-section. By carefully selecting the geometric parameters of the VCM, one can intelligently shape the overall VCM PDF.

III. Facility Sputtering Model

As a case study, Georgia Institute of Technology’s VTF-2 electric propulsion chamber was selected as a test geometry due to its involvement in the JANUS project. NASA’s Hall Effect Rocket with Magnetic Shielding (HERMeS) 12.5 kW thruster was selected as the test article of interest; its plume profile at 300 eV was extracted from Kamhawi et al. and imported into the VTF-2 geometry.²² A simplified model of the simulation domain is shown in Fig. 3, depicting the Hall-effect thruster (HET) location, the plume profile, and the numbered panel collectors. The chamber walls, beam dump, thruster, and pumps are divided into 46 individual surfaces, mirrored about the central axis, in order to create particle collection statistics (i.e., particles collected on surface number 2 include both the upper and lower panels). For this study, the areas referred to the beam target include the central conical structure on the downstream end of the chamber (numbered surfaces 1 and 2), the adjoining back wall (numbered surfaces 3 through 6), as well as the angled flat plates (numbered surfaces 42 and 43).

Beam target surfaces, highlighted in red in Fig. 3, are graphite GR060, while all other surfaces are stainless steel 304 (SS304), including the pump faces. Due to material limitations in the TRI3DYN software, the graphite surfaces and SS304 are approximated as amorphous carbon and iron, respectively. The parameter of surface binding energy for these materials were calibrated against data from Tartz and Neumann²³ (2007), Kolasinski et al.²⁴ (2009), and Polk²⁵ (2024) for carbon, and Williams and Corey²⁶ (2010) for iron.

Xenon particles are generated at the outlet face of the thruster with an energy of 300 eV, with their initial direction selected based on a weighted probability derived from the imported HERMeS HET profile. These particles are then tracked as they interact with the beam target and chamber surfaces to study the transport

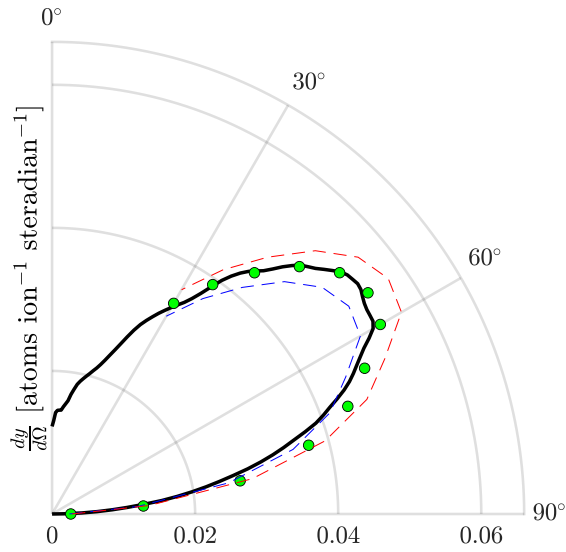


Figure 2: Experimental PDF of 65% RD, 65 PPI stochastic tungsten VCM (green points) overlaid with TRI3DYN result of normal incidence xenon ions at 150 eV. Error bars on the experimental data are depicted as dashed lines.

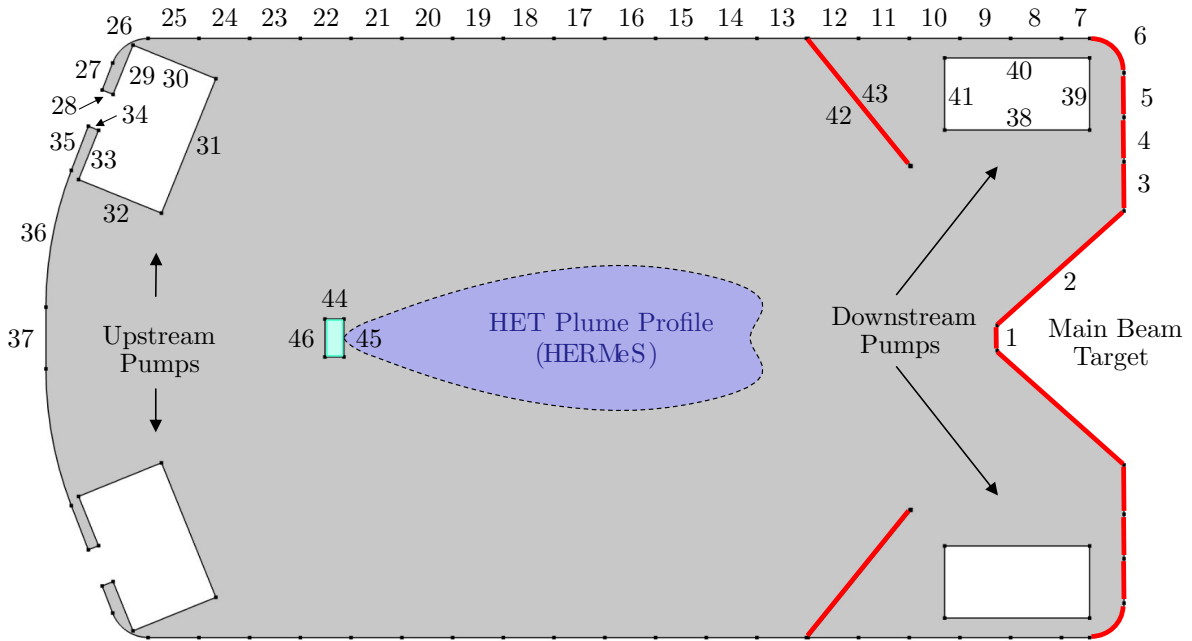


Figure 3: Georgia Tech VTF-2 chamber. Beam target surfaces highlighted in red.

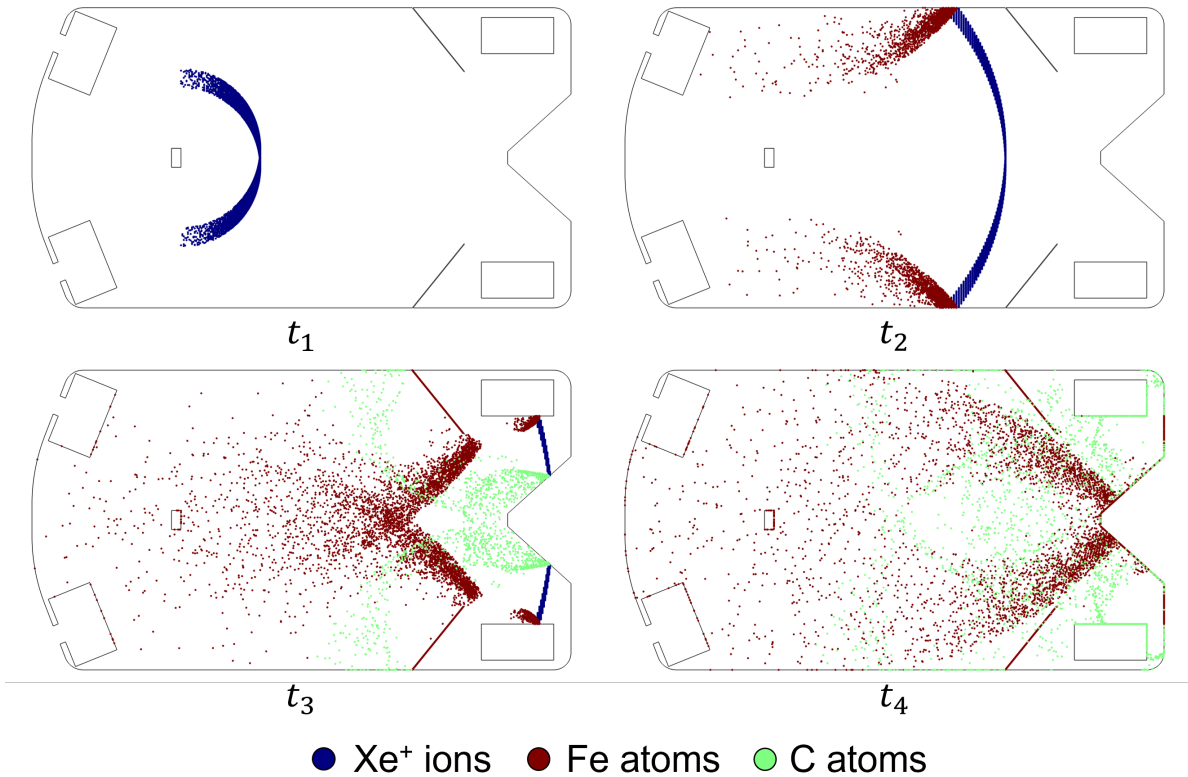


Figure 4: Time series of HERMeS hall thruster plume comprised of 100k xenon ions with energies of 300 eV interacting with Georgia Tech’s VTF-2 steel chamber walls and carbon beam target.

of sputtered material from during operation, and track the accumulation of material on key surfaces (see Fig. 4).

It is assumed that once an ion liberates a sputtered atom, the resulting energy of the resulting sputterant is insufficient to cause further sputtering.²⁷ Therefore, once created, all sputterants will travel within the open space of the domain until they encounter a surface. The final number of sputterants, and their elemental composition can then be calculated for each surface of the geometry, and a map of transported material is generated. The model can simulate the transport of 1 million initial ions in roughly 5 minutes. This number of particles was chosen so as to reduce variation of accumulated particles between runs to less than 1%.

IV. Results and Analysis

Six separate variations of chamber design were considered for this study, which utilize the strategic placement of flat carbon and carbon VCMs throughout key surfaces in the VTF-2 chamber, outlined in Table 1. In addition to stochastic foam carbon VCMs, an advanced manufactured (AM) carbon VCM, similar to that presented by Sabiston and Wirz,²¹ is included. This AM carbon VCM combines the sputter yield reduction of the stochastic carbon foam VCM, but possesses the directional PDFs of flat carbon, which vary as a function of incidence angle. In this way, the AM VCM can be thought of as a “direction-preserving” optimized lattice structure. Pictograms are inset in the tables to aid in identifying case geometry. Red half-cylinders indicate that the chamber walls for that geometry were set to steel, while black indicates flat carbon, the open cell foam pattern indicates stochastic carbon foam VCM, and the regularized mesh pattern indicates AM carbon VCM. A reduction in sputter yield for both VCM types was assumed to be $\frac{Y}{Y_0} = 0.5$, where Y is the VCM yield, and Y_0 is the yield from a flat surface, at normal incidence.^{13, 15} Additionally, the pumps are set to possess steel material properties; this property is not altered for any simulation configuration. In fact, in the B series of cases where all chamber walls and beam target surfaces are some form of carbon, the pumps remain a leading source of sputterants in the chamber (as well as being the only source of steel

sputterants).

Tables 2 through 5 have two separate columns for comparison of sputter yield reduction for various surfaces. The column with header “A.1 Baseline” uses the current VTF-2 geometry (flat carbon beam target surfaces and steel walls) as the simulation to compare against. A second column with header “B.1 Baseline” is included, as when comparing cases where the entirety of the inner surface of the chamber is a single material (i.e., stochastic foam VCM, or AM VCM), using the B.1 case as baseline - wherein all surfaces are flat carbon - is also an instructive comparison to make. The final column contains information on what percentage of the collected sputterants for the surface under consideration are composed of carbon, as opposed to steel.







Case Group	Case	Description
A - Steel Walls	A.1 	Flat carbon beam target [VTF-2 Baseline]
	A.2 	Stochastic carbon foam VCM beam target
	A.3 	Advanced manufactured carbon VCM beam target
B - Carbon/VCM walls	B.1 	All flat carbon surfaces
	B.2 	All stochastic carbon foam VCM surfaces
	B.3 	All advanced manufactured carbon VCM surfaces

Table 1: Simulated VTF-2 chamber material configurations.

A. General Findings

Firstly, the baseline simulation (A.1) suggests that with the current VTF-2 chamber configuration of steel walls and flat carbon beam target surfaces, more than half of the total sputtered particles that are generated from the ion plume are composed of steel rather than carbon (see Table 2). While the the majority of the plume impacts carbon surfaces, the ions on the wings of the distribution that do impact the chamber wall produce a comparatively large number of sputterants. While this finding is not necessarily unexpected, as the sputter yield of steel is an order of magnitude higher than carbon at normal incidence, it does highlight the importance of material selection for electric propulsion facility effects, and the outsized contribution of sputter yield from non-beam target surfaces.

The inclusion of VCMs as beam target and chamber wall materials have profound effects on the total sputter yield in the chamber. For instance, in this study, the sputter yield of carbon VCMs were selected to be on order of 50% of the normal yield for flat carbon, in agreement with literature.^{13,15} However, because the sputter yield for a non-normal incidence on a flat carbon surface can be up to 5 times the normal incidence yield,²⁴ the total number of sputterants produced can be reduced far beyond 50% of baseline. In fact, compared to the VTF-2 baseline configuration (A.1), a carbon VCM beam target (A.2/A.3) reduces the total number of carbon sputterants in the chamber by nearly 70%.

Figure 5 and Figure 6 present heat maps showing the percentage difference in collected particles on chamber surfaces for cases A.2/A.3 and B.2/B.3, respectively. For these heat maps, case A.1 was used as a baseline, in an effort to showcase the gains that can be made in sputter yield reduction compared to the current design of the VTF-2 chamber.





Case	Total Sputterant Reduction		Carbon Percentage
	A.1 Baseline	B.1 Baseline	
A.1 	—	—	43.0%
A.2/A.3 	31.2%	—	19.0%
B.1 	22.2%	—	58.8%
B.2/B.3 	54.6%	41.6%	30.2%

Table 2: Reduction in total created sputterants to all chamber surfaces.







Case	Thruster Sputterant Reduction		Carbon Percentage
	A.1 Baseline	B.1 Baseline	
A.1 	—	—	44.2%
A.2 	-14.3%	—	55.2%
A.3 	32.1%	—	31.6%
B.1 	43.4%	—	95.0%
B.2 	28.9%	-25.5%	95.3%
B.3 	76.1%	57.7%	86.0%

Table 3: Reduction in sputterants to thruster face. Increases in collected sputterants to thruster surfaces are highlighted in red.







Case	Downstream Pump Sputterant Reduction		Carbon Percentage
	A.1 Baseline	B.1 Baseline	
A.1 	—	—	82.4%
A.2 	68.1%	—	46.9%
A.3 	57.8%	—	58.1%
B.1 	15.6%	—	100%
B.2 	84.8%	82.0%	99.1%
B.3 	74.8%	70.2%	100%

Table 4: Reduction in sputterants to downstream pumps.







Case	Upstream Pump Sputterant Reduction		Carbon Percentage
	A.1 Baseline	B.1 Baseline	
A.1 	—	—	64.7%
A.2 	-14.2%	—	73.0%
A.3 	39.1%	—	42.5%
B.1 	30.2%	—	94.8%
B.2 	7.6%	-32.4%	94.4%
B.3 	68.6%	54.9%	80.0%

Table 5: Reduction in sputterants to upstream pumps. Increases in collected sputterants on upstream pump surfaces are highlighted in red.

B. Case A Series - Varying beam target material, maintain steel chamber walls

In comparing the baseline VTF-2 (A.1) geometry with the VCM beam target cases (A.2/A.3), both the stochastic foam and AM VCMs reduce the total number of generated sputterants by the same amount, around 31.2%, as they share the same sputter yield, irrespective of incidence angle (see Table 2). Interestingly, results from Table 3 show that the stochastic foam VCM increases the material that is captured on the thruster surfaces (an increase of 14.3%). While the stochastic foam VCM surfaces do serve to reduce the total number of sputterants that leave the material, the trajectories that these sputtered particles take have the potential to more preferentially be directed back towards the thruster face. For example, the PDFs that sputtered atoms largely assume when coming into contact with the flat carbon conical beam target are directed towards the back wall, and the pumps, due to the forward-scattering nature of the ion-solid interaction. This limits the probability of these carbon atoms being directed back upstream, towards the thruster. However, in the case of the stochastic carbon foam VCM, the PDF is in the form of a symmetric under-cosine, normal to the surface of the VCM; this causes a “lobe” of the PDF to be directed backwards to the thruster, given the

current angled geometry of the conical beam target. The AM VCM, which preserves the flat carbon PDFs, but possesses the preferable sputter yield reduction factor, reduces the amount of material on the thruster face by 32.1%. Regarding the material accumulated on the pump surfaces, the downstream pumps both see a marked decrease, on the order of 58% to 68% less (see Table 4), while the upstream pumps experience an increase in sputterants for the stochastic foam VCM case, and a decrease for the AM VCM, for the same reasons as in the case of the thruster sputter transport (see Table 5).

C. Case B Series - Varying beam target and chamber wall material

When the interior surfaces of the chamber walls are also set to possess carbon material properties, its inherently low sputter yield causes further reductions of total sputtered material in the chamber; especially when considering that in the baseline (A.1) case, more than half of the sputterants originate from the steel chamber walls. As shown in Table 2, reductions on the order of 22.2% can be found for flat carbon, with further reductions up to 54.6% for the VCMs (due to the VCM sputter yield remaining unchanged with increasing incidence angle).

By choosing to coat the chamber walls with flat carbon (B.1), sputterants collected on the thruster can be expected to be reduced by 43.4% (Table 3) compared to baseline (A.1), with slightly smaller reductions to the upstream and downstream pumps. This is an economical option when considering cost-effective, non-invasive methods to minimize sputterants to the thruster surfaces, pumps, and generally within the chamber. For further reductions in sputterants to critical surfaces, the AM VCMs seem to have an advantage over the stochastic foam VCMs; the PDFs produced by the stochastic foams have the same effect as in the A series of cases, shuttling sputtered material to the thruster faces and pumps (more specifically, the upstream pumps). However, if stochastic foam VCMs were to be added to the VTF-2 chamber, a more reasonable geometry would likely include reducing the angle of the conical beam target, to push the lobes of the under-cosine PDF away from the thruster, and towards the back wall.

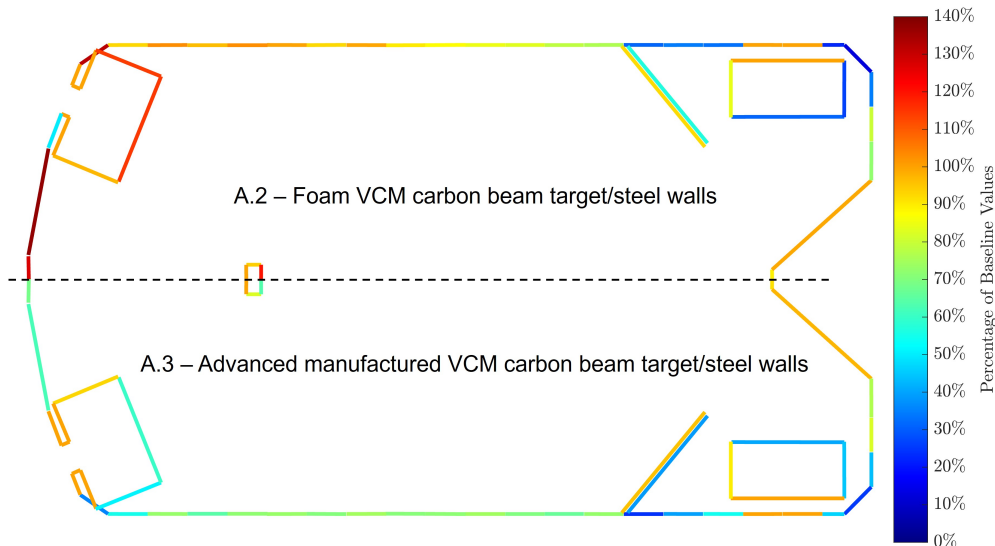


Figure 5: Heatmap of surface collectors for simulation cases A.2 and A.3, illustrating the total collected sputterants on each panel, as a percentage of the baseline case, A.1.

V. Conclusion and Future Work

A new computational tool for simulating sputtering transport mechanisms in electric propulsion test facilities was developed, providing insights into best practices for beam target design. The main takeaways

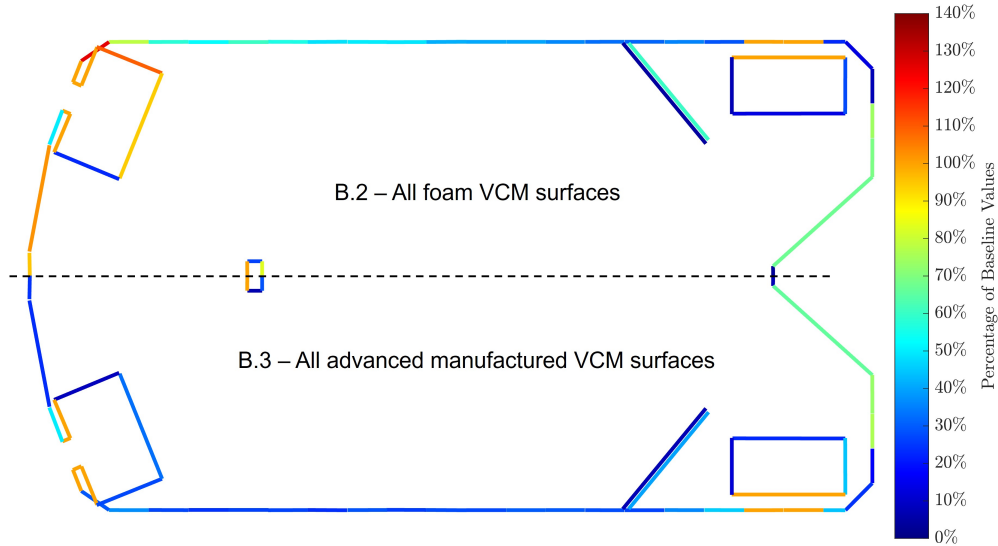


Figure 6: Heatmap of surface collectors for simulation cases B.2 and B.3, illustrating the total collected sputterants on each panel, as a percentage of the baseline case, A.1.

are summarized as follows:

- The impact of volumetrically complex materials on reducing sputtering within electric propulsion test facilities was found to be significant, but care must be taken when selecting both the placement and type of sputter-reducing material on EP test facility surfaces.
 - The altered PDFs of stochastic foam VCMs were found to produce a surplus of sputtered carbon that was deposited on critical test surfaces compared to the baseline chamber geometry.
 - Advanced manufactured VCMs that combine the reduced sputter yield of stochastic foam VCMs with directionality-preserving sputtering behavior found in flat materials are the superior option for minimizing total sputterants to critical surfaces in the chamber.
 - Reductions in the unwanted effects of ion-induced electron emission and secondary electron emission in VCMs are proportional to reductions in sputtering.^{16–18}
- The contribution of ions from the edges of the HET plume sputtering the steel chamber walls was found to make up more than half of the total sputterants created in the baseline geometry case.
 - Changing these steel wall surfaces to flat carbon is a simple, cost-effective method to dramatically reduce sputterants in the chamber.

The findings suggest that VCMs, due to their low sputter yield and geometric trapping capabilities, are a promising solution for enhancing the longevity and performance of electric propulsion systems. Future work will focus on optimizing the geometric properties of VCMs to control the PDFs of sputtered material, including effects of back-scattered ions and background neutral density,²⁸ and refining the precision TRI3DYN simulations to include effects of ion implantation and damage.²⁷

References

¹ Antonio Piragino, Farbod Faraji, Maryam Reza, Eugenio Ferrato, Annalisa Piraino, and Tommaso Andreussi. Background pressure effects on the performance of a 20 kw magnetically shielded hall thruster operating in various configurations. *Aerospace*, 8(3):69, 2021.

- ²James E Polk, O Duchemin, Chih-Sung Ho, and BE Koel. The effect of carbon deposition on accelerator grid wear rates in ion engine ground testing. 2000.
- ³Daniel Herman, George Soulas, and Michael Patterson. Next long-duration test plume and wear characteristics after 16,550 h of operation and 337 kg of xenon processed. In *44th AIAA/ASME/SAE/ASEE Joint Propulsion Conference & Exhibit*, page 4919, 2009.
- ⁴Mitchell LR Walker, Dan Lev, Maryam Saeedifard, Benjamin Jorns, John Foster, Alec D Gallimore, Alex Gorodetsky, Joshua L Rovey, Huck Beng Chew, Deborah Levin, et al. Overview of the joint advanced propulsion institute (janus). In *37th International Electric Propulsion Conference*, 2022.
- ⁵Hongru Zheng, Guobiao Cai, Lihui Liu, Shengfei Shang, and Bijiao He. Three-dimensional particle simulation of back-sputtered carbon in electric propulsion test facility. *Acta Astronautica*, 132:161–169, 2017.
- ⁶Keita Nishii, Sean Clark, Joshua Tompkins, Nakul Nuwal, Deborah A Levin, and Joshua L Rovey. Numerical simulation of carbon sputtering for electric propulsion in the ground facility. In *37th International Electric Propulsion Conference Massachusetts Institute of Technology, Cambridge, MA, USA, IEPC-2022*, volume 379, 2022.
- ⁷Samuel J Araki, Robert S Martin, David L Bilyeu, Lubos Brieda, Carrie Hill, and Maria Choi. Current capabilities of ari1’s spacecraft simulation tool. In *37th International Electric Propulsion Conference*, 2022.
- ⁸Revathi Jambunathan and Deborah A Levin. Chaos: An octree-based pic-dsmc code for modeling of electron kinetic properties in a plasma plume using mpi-cuda parallelization. *Journal of computational physics*, 373:571–604, 2018.
- ⁹Huy D Tran, Sean A Clark, Reed Thompson, Deborah A Levin, Joshua L Rovey, and Huck Beng Chew. Carbon transport in electric propulsion testing-i: Multiscale computations for carbon sputtering by low energy ion bombardment. In *AIAA SCITECH 2024 Forum*, page 1135, 2024.
- ¹⁰Samuel J. Araki and Robert S. Martin. Sputtered atom transport calculation via radiosity view factor model and particle data compression. *Vacuum*, 210:111867, 2023.
- ¹¹Y Yamamura and Shigeru Shindo. An empirical formula for angular dependence of sputtering yields. *Radiation effects*, 80(1-2):57–72, 1984.
- ¹²Graeme Sabiston and Richard E Wirz. Volumetrically complex materials for reducing electric propulsion facility effects. 2022.
- ¹³Graeme Sabiston and Richard E Wirz. Ion–surface interactions in plasma-facing material design. *Journal of Applied Physics*, 135(18), 2024.
- ¹⁴Wolfhard Möller. Tri3dyn–collisional computer simulation of the dynamic evolution of 3-dimensional nanostructures under ion irradiation. *Nuclear Instruments and Methods in Physics Research Section B: Beam Interactions with Materials and Atoms*, 322:23–33, 2014.
- ¹⁵Gary Z Li and Richard E Wirz. Persistent sputtering yield reduction in plasma-infused foams. *Physical Review Letters*, 126(3):035001, 2021.
- ¹⁶Angelica Ottaviano and Richard E Wirz. Secondary electron emission of reticulated foam materials. *Journal of Applied Physics*, 133(10), 2023.
- ¹⁷Jorge Fernandez-Coppel, Richard Wirz, and Jaime Marian. Fully discrete model of kinetic ion-induced electron emission from metal surfaces. *Journal of Applied Physics*, 135(8), 2024.
- ¹⁸MI Patino and RE Wirz. Electron emission from carbon velvet due to incident xenon ions. *Applied Physics Letters*, 113(4), 2018.
- ¹⁹Gary Zhi Li. *Plasma sputtering behavior of structured materials*. University of California, Los Angeles, 2020.
- ²⁰Oleg V Sazhin, Sergei F Borisov, and Felix Sharipov. Accommodation coefficient of tangential momentum on atomically clean and contaminated surfaces. *Journal of Vacuum Science & Technology A: Vacuum, Surfaces, and Films*, 19(5):2499–2503, 2001.
- ²¹Graeme T Sabiston and Richard E Wirz. Thrust densification of space electric propulsion systems via volumetrically complex materials. In *AIAA SCITECH 2024 Forum*, page 1136, 2024.
- ²²Hani Kamhawi, Wensheng Huang, James H Gilland, Thomas W Haag, Jonathan Mackey, John Yim, Luis Pinero, George Williams, Peter Peterson, and Daniel Herman. Performance, stability, and plume characterization of the hermes thruster with boron nitride silica composite discharge channel. In *International Electric Propulsion Conference (IEPC 2017)*, number GRC-E-DAA-TN46397, 2017.
- ²³Michael Tartz and Horst Neumann. Sputter yields of carbon materials under xenon ion incidence. *Plasma Processes and Polymers*, 4(S1):S633–S636, 2007.
- ²⁴Robert D Kolasinski, James E Polk, Dan Goebel, and Lee K Johnson. Carbon sputtering yield measurements at grazing incidence. *Applied Surface Science*, 254(8):2506–2515, 2008.
- ²⁵James E Polk. A critical review and meta-analysis of xenon-on-carbon sputter yield data. *Journal of Applied Physics*, 135(4), 2024.
- ²⁶John D Williams and Ronald L Corey. Influence of residual gases on witness plate measurements during hall-effect thruster testing. *Plasma Sources Science and Technology*, 19(2):025020, 2010.
- ²⁷Luke K. Franz and Richard E Wirz. Xe-c scattering, implantation, and sputtering analysis for ep systems. In *International Electric Propulsion Conference*, number IEPC-2024-552, 2024.
- ²⁸Ehsan Taghizadeh and Richard E Wirz. Reduced order modeling and optimization for electric propulsion vacuum chambers. In *International Electric Propulsion Conference*, number IEPC-2024-588, 2024.